Electronic Supplementary Material (ESI) for Journal of Materials Chemistry A.

Supporting Information

Facile regrowth of Mg-Fe_2O_3/P-Fe_2O_3 homojunction photoelectrode for efficient solar water oxidation

Feng Li [a], Jing Li [a], Fengwang Li [b], Lili Gao [a], Xuefeng Long [a], Yiping Hu [a],

Chenglong Wang [a], Shenqi Wei [a], Jun Jin [a*] and Jiantai Ma [a*].

1. The equations

The conversion between potentials versus Ag/AgCl and versus RHE is determined using the equation below.

$$E(\text{versus RHE}) = E(\text{versus Ag/AgCl}) + E_{\text{Ag/AgCl}}(\text{refer}) + 0.0591\text{V} \times \text{pH}$$

$$E_{\text{Ag/AgCl}}(\text{refer}) = 0.197\ \text{V versus NHE at } 25\ ^{\circ}\text{C} \qquad (1)$$

Incident photon to current efficiency (IPCE) was obtained using an Oriel Cornerstone 260 1/4 m monochromator with a 500W Oriel Xe lamp as the simulated light source (LSH-X500B). An applied potential of 1.23 V vs. RHE was supplied by a miniature integrated electrochemical workstation (Zolix Instruments Co., Ltd). IPCE values were calculated using the equation below

$$IPCE(\%) = \frac{J \times 1240}{\lambda \times P_{light}} \times 100\% \qquad (2)$$

J refers to the photocurrent density (mA cm^{-2}) obtained from the electrochemical workstation. λ and P_{light} are the incident light wavelength (nm) and the power density obtained at a specific wavelength (mW cm^{-2}), respectively.

Applied bias photon-to-current efficiency (ABPE) can be calculated using the following equation:

$$ABPE(\%) = \frac{J \times (1.23 - V_b)}{P_{light}} \times 100\% \qquad (3)$$

J refers to the photocurrent density (mA cm^{-2}) obtained from the electrochemical workstation. V_b is the applied bias vs. RHE (V), and P_{light} is the total light intensity of AM 1.5 G (100 mW cm^{-2}).

The light absorption efficiency or light harvesting efficiencies (LHE, defined as the ratio of absorbed light to the incident light) of each photoanodes are calculated from their UV−Vis absorption spectra:

$$LHE = 1 - 10^{-A(\lambda)} \qquad (4)$$

where A(λ) is the absorbance at a specific wavelength. In order to calculate J_{abs} (the photocurrent density achievable assuming 100% absorbed photon–to–current conversion efficiency for photons) the solar spectral irradiance at AM 1.5G ($W \cdot m^{-2} \cdot nm^{-1}$, ASTM G173−03) is first converted to solar photocurrents vs. wavelength ($A \cdot m^{-2} \cdot nm^{-1}$) assuming 100% IPCE for photons. Then the solar photocurrents are multiplied by the LHE at each wavelength and adding these products up.

According to the M-S curves, charge carrier density (N_d) can be calculated using the following equation:

$$N_d = \frac{2}{e\varepsilon_0\varepsilon} \times \left[\frac{d\left[\frac{1}{C^2}\right]}{dV_S} \right]^{-1} \qquad (5)$$

The electronic charge (e) is 1.6 × 10^{-19} C, vacuum permittivity (ε_0) is 8.854×10^{-14} F m^{-1}, and relative permittivity (ε) is 80 for hematite [1]. C (F cm^{-2}) is the space charge capacitance in the semiconductor (obtained from M-S curves), and V_s (V) is the applied potential for M-S curves.

the efficiency of charge transport in the bulk (η_{bulk}, relating to bulk charge separation) and surface charge transfer efficiency ($\eta_{surface}$, the yield of holes that are involved in water oxidation reaction after reaching the electrode/electrolyte interfaces) of the prepared photoanodes, can be calculated using the following equations:

$$\eta_{bulk} = \frac{J^{Na_2SO_3}}{J_{abs}} \qquad (6)$$

$$\eta_{surface} = \frac{J^{H_2O}}{J^{Na_2SO_3}} \qquad (7)$$

J_{abs} is the unity converted photocurrent density from the light absorption, while J^{H2O} and J^{Na2SO3} are the photocurrent densities obtained in 1 M KOH electrolyte and 1 M Na_2SO_3 (pH 9.5), respectively[2].

The water oxidation efficiency (η_{OER}) is calculated by the following equation.

$$\eta_{OER} = \frac{K_{ct}}{K_{ct} + K_{rec}} = \frac{R_{Bull}}{R_{Bull} + R_{ct}} \qquad (8)$$

Where K_{ct} is the charge transfer rate constant, K_{rec} is the rate constant. And the EIS data of R_{Bulk} and R_{ct} is fitted by the ZView software.

2. DFT Calculations (method and model)

The $Fe_{48}O_{68}$ with oxygen vacancy concentration of 3.33%, $Fe_{47}MgO_{69}$ and $Fe_{46}P_2O_{68}$ have been built. The first principles calculations in the framework of density functional theory, including structural, electronic and optical performances, were carried out based on the Cambridge Sequential Total Energy Package known as CASTEP [3]. The exchange–correlation functional under the generalized gradient approximation (GGA)[4] with norm-conserving pseudopotentials and Perdew–Burke–Ernzerhof functional was adopted to describe the electron–electron interaction [5]. An energy cutoff of 750 eV was used and a k-point sampling set of 3 x 6 x 4 were tested to be converged. A force tolerance of 0.01 eV $Å^{-1}$, energy tolerance of 5.0×10^{-7}eV per atom and maximum displacement of 5.0×10^{-4} Å were considered. Each atom in the storage models is allowed to relax to the minimum in the enthalpy without any constraints. The GGA+U approach, which introduces an intra-atomic electron–electron interaction as an on-site correction to describe systems with localized *d* and *f* states, can produce more precise band gap than GGA[6, 7]. To account for the strongly correlated interactions among the Fe 3*d* electrons and calculate the electronic structures, a moderate on-site Coulomb repulsion $U = 5.5$ eV is applied.

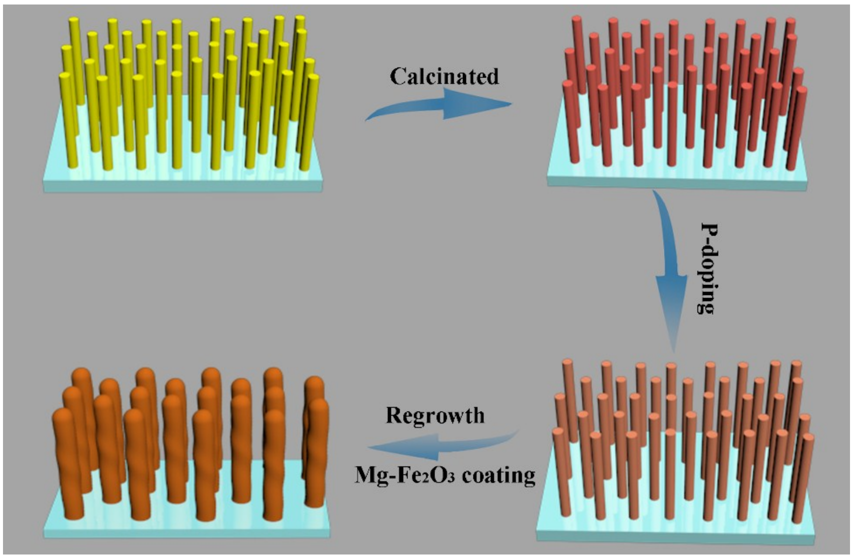

Scheme S1. Schematic diagram of the preparation procedure of the Mg-Fe_2O_3/P-Fe_2O_3 NRs photoanode

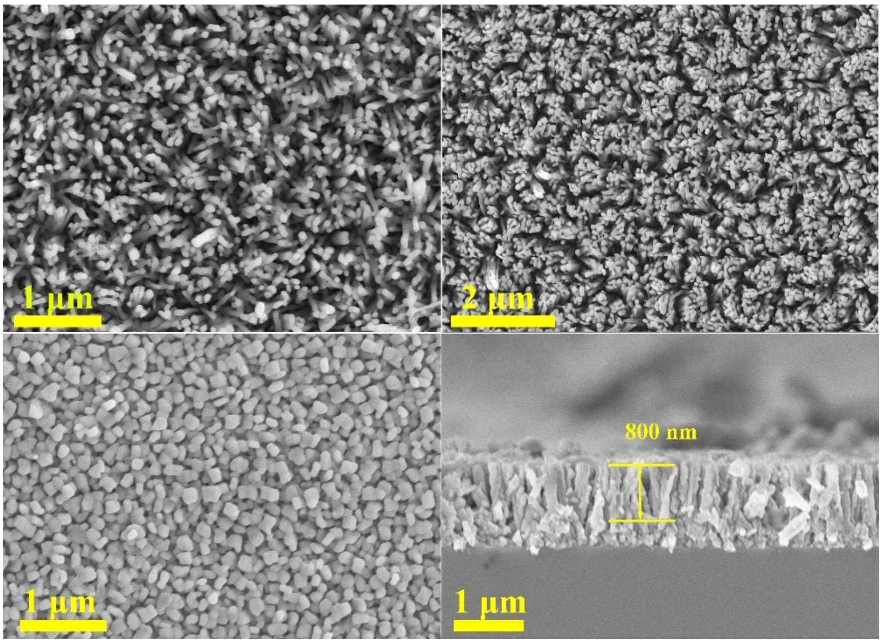

Figure S1. Top-view SEM images of (a) α-Fe_2O_3, (b) P-Fe_2O_3, (c) Mg-Fe_2O_3/P-Fe_2O_3 NRs and cross-section SEM image of Mg-Fe_2O_3/P-Fe_2O_3 (d)

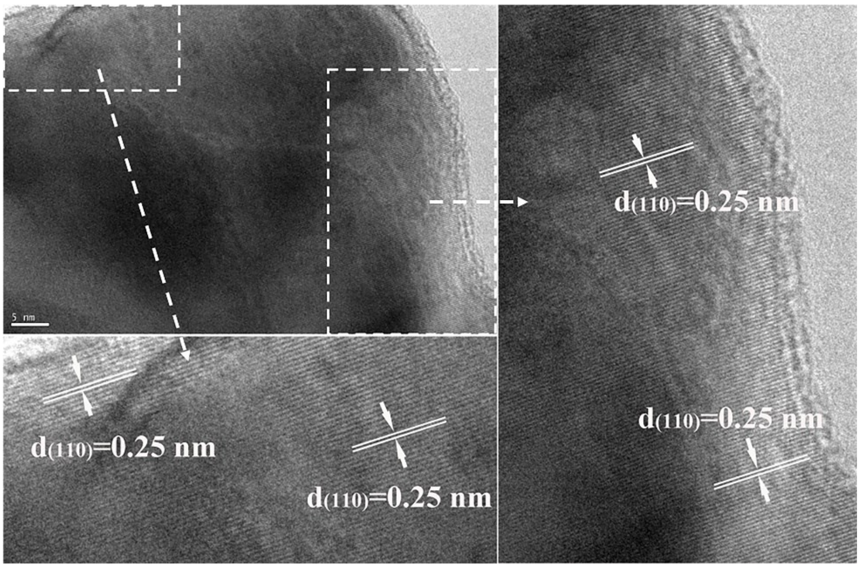

Figure S2. HRTEM images of Mg-Fe_2O_3/P-Fe_2O_3.

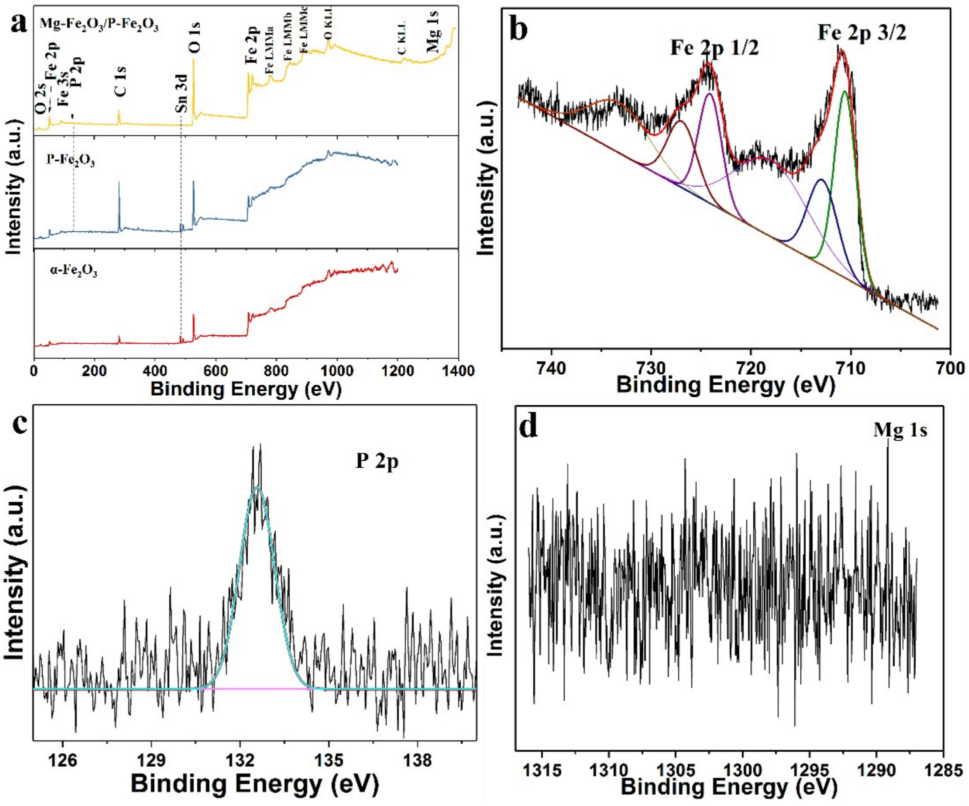

Figure S3. a) XPS survey spectrum of α-Fe_2O_3, P-Fe_2O_3 and Mg-Fe_2O_3/P-Fe_2O_3 NRs photoanodes, XPS high resolution (b) Fe 2p, (c) P 2p and (d) Mg 1s of Mg-Fe_2O_3/P-Fe_2O_3 NRs photoanode.

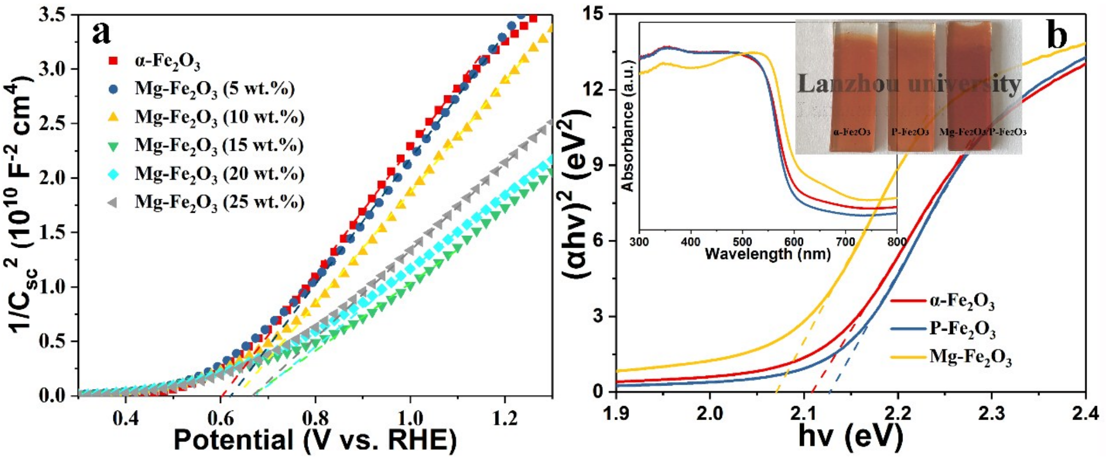

Figure S4. (a) Mott–Schottky plots of Mg-Fe_2O_3 with different content of Mg precursor collected at a fixed frequency of 1 kHz, (b) UV–visible absorption spectrum spectra of each photoanode.

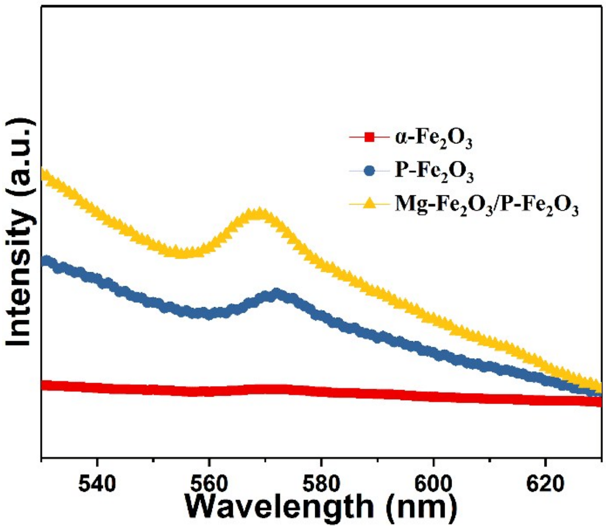

Figure S5. Photoluminescence (PL) spectra of each photoanodes.

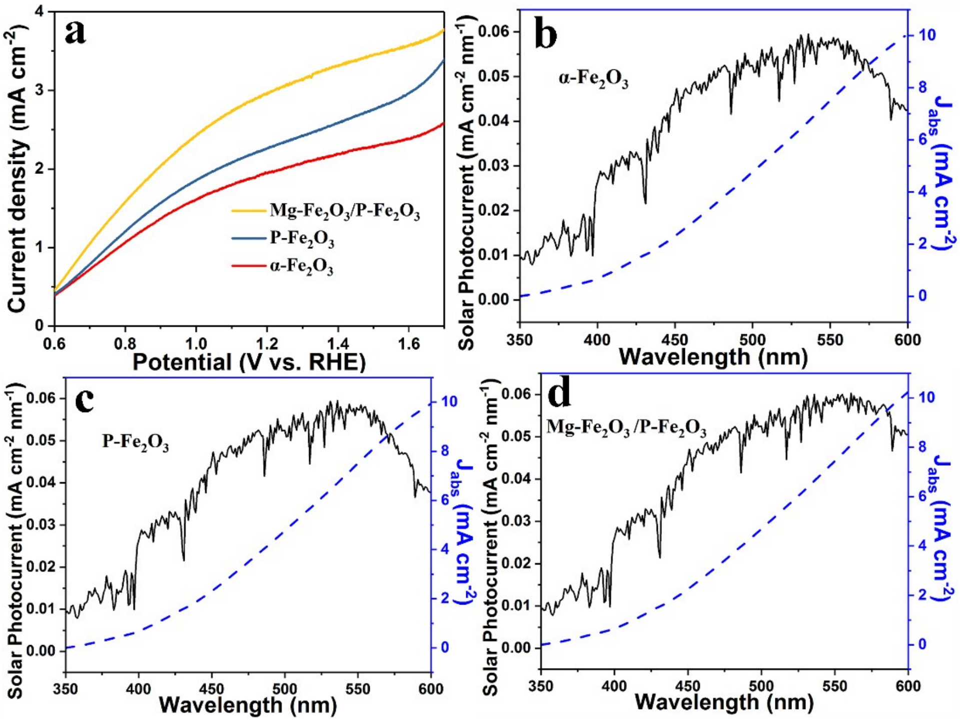

Figure S6. (a) LSVs of each photoanode collected at 5 mV s^{-1} in a 0.5 M Na_2SO_3 aqueous electrolyte under one sun illumination (100 mW cm^{-2}), Jabs values of (b) α-Fe_2O_3, (c) P-Fe_2O_3 and (d) Mg-Fe_2O_3/P-Fe_2O_3 NRs photoanodes (assuming 100% absorbed photon-to-current conversion efficiency for photons).

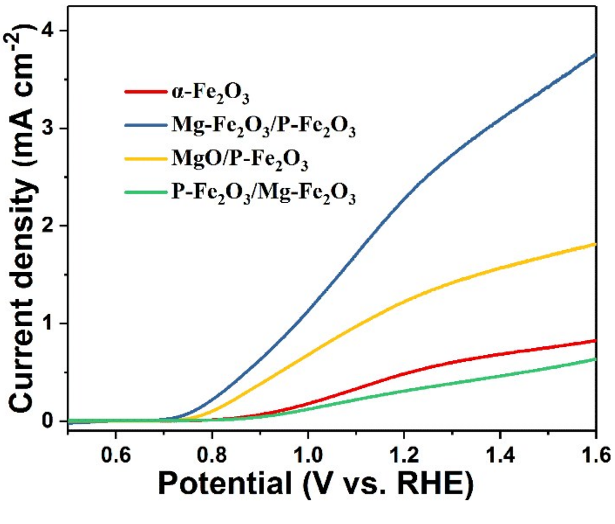

Figure S7. Photocurrent density vs. applied potential curves for each sample.

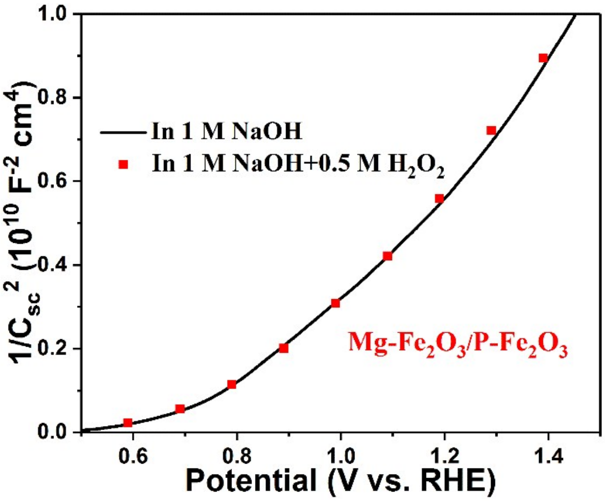

Figure S8. Mott–Schottky plots of the Mg-Fe_2O_3/P-Fe_2O_3 NRs photoanodes measured at a frequency of 1000 Hz in 1 M NaOH solution with or without a hole scavenger (0.5 M H_2O_2)

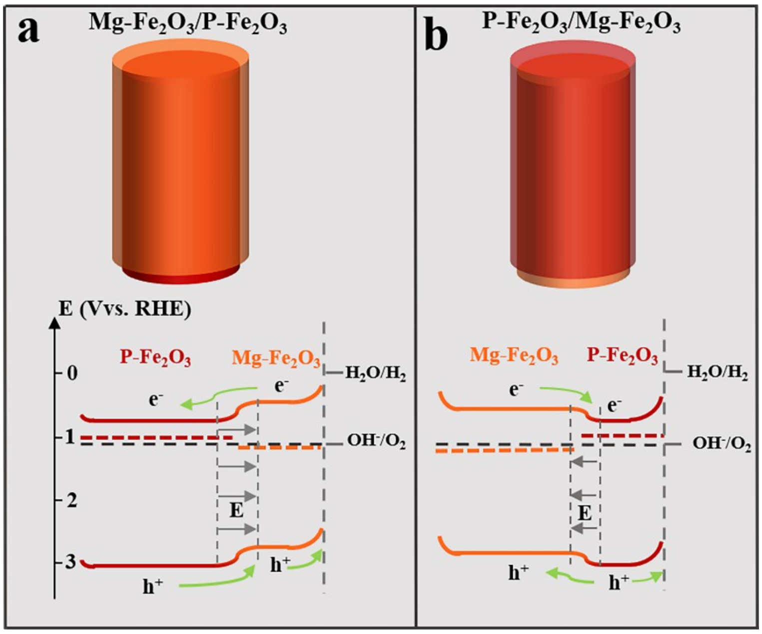

Figure S9. Energy band diagrams of (a) Mg-Fe_2O_3/P-Fe_2O_3 NRs and (b) P-Fe_2O_3/Mg-Fe_2O_3 NRs in solution.

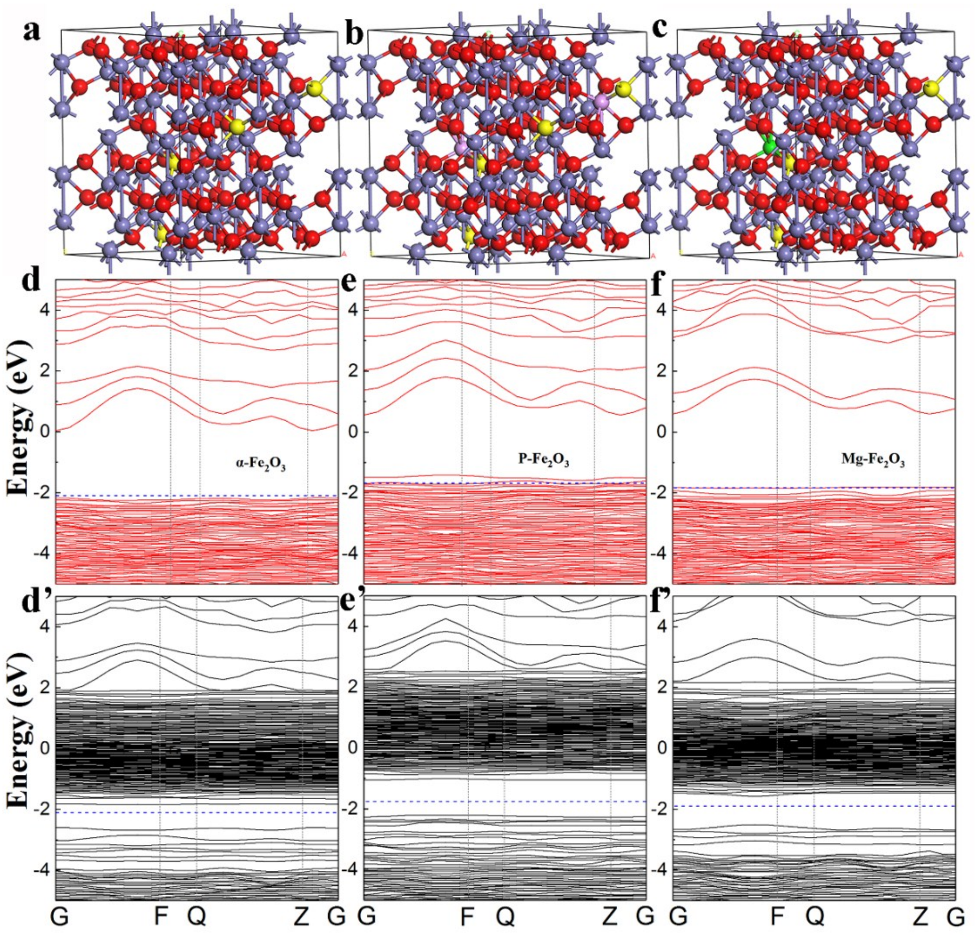

Figure S10. The optimized structure of (a) α-Fe_2O_3 ($Fe_{48}O_{68}$ with oxygen vacancy concentration of 3.33%), (b) P-Fe_2O_3 ($Fe_{46}P_2O_{68}$) and (c) Mg-Fe_2O_3 ($Fe_{47}MgO_{69}$) (yellow atom: Oxygen vacancy; Purple atoms: P; Green atoms: Mg.) during the calculation. Band structures of of (d, d') α-Fe_2O_3, (e, e') P-Fe_2O_3 and (f, f') Mg-Fe_2O_3. Red line: spin-up; black line: spin-down states. The highest occupied state is set to Femi level.

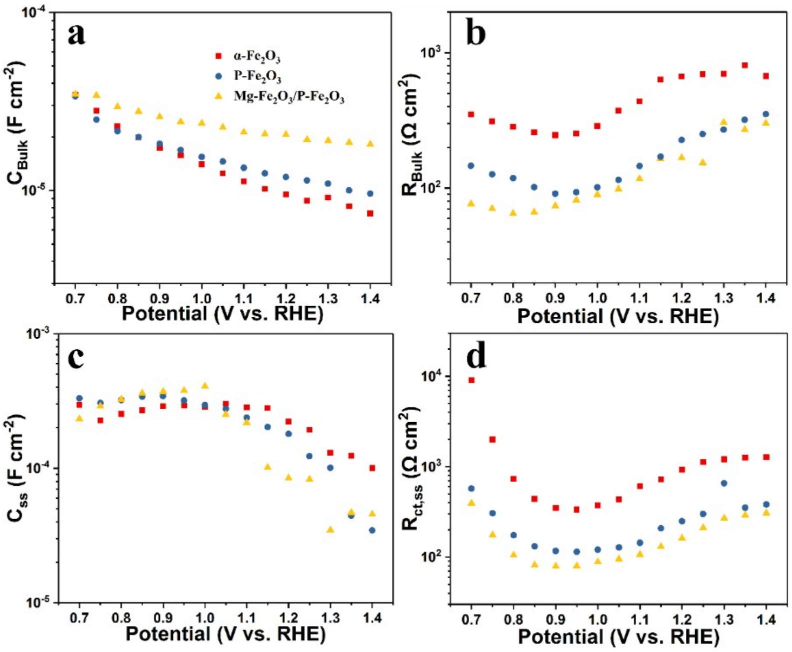

Figure S11. (a) C_{Bulk}, (b) R_{Bulk} (c) C_{ss} and (d) $R_{ct,\ ss}$ based on the equivalent circuit at different potentials of the each photoanode.

Table S1. Atomic contents from the surface of the samples obtained from XPS.

Sample	Element	Raw Area (cps eV)	RSF	Atomic Conc %	Mass Cond %
$Mg\text{-}Fe_2O_3/P\text{-}Fe_2O_3$	**Fe 2p**	65368.4	2.957	**29.84**	56.08
	O 1s	39951.8	0.780	**67.65**	38.37
	P 2p	588.0	0.486	**1.67**	1.83
	Mg 1s	2101.1	2.260	**0.84**	0.72
$P\text{-}Fe_2O_3$	**Fe 2p**	43738.9	2.957	**33.26**	62.76
	O 1s	22854.1	0.780	**64.46**	34.85
	P 2p	484.2	0.486	**2.29**	2.39
$\alpha\text{-}Fe_2O_3$	**Fe 2p**	21058.6	2.957	**41.38**	71.13
	O 1s	8044.2	0.780	**58.62**	28.87

Table S2 Comparison of our photoanode to other α-Fe_2O_3-based photoanod

Catalyst	The onset potential (V vs.RHE)	Current density at 1.23 V vs. RHE (mA cm^{-2})	IPCE value (%)	Ref.
Mg-Fe_2O_3/P-Fe_2O_3	0.68	2.4	36 at 1.23V (300 nm)	This work
grad-P:Fe_2O_3/Co-Pi	0.8	2.0	28 at 1.23V (360 nm)	*Chem. Sci.*, 2017, 8, 91–100
FeOOH/ Fe_2O_3	0.65	1.21	no	*Angew. Chem. Int. Ed.* 2016, 55, 10854
Zr-Fe_2O_3 NT	~ 0.89	1.50	25.7 at 1.23V (370 nm)	*Angew. Chem. Int. Ed.* 2017, 129, 1 – 7
Rh−F-Fe_2TiO_5/ Fe_2O_3	0.63	2.12	37 at 1.25V (370 nm)	*ACS Catal.* 2017, 7, 4062−4069
C coated Fe_2O_3	0.77	2.0	no	*Appl. Catal. B-Environ.*, 2017, 207, 1–8
C/Co_3O_4−Fe_2O_3	0.77	1.48	28 at 1.23V (325 nm)	*Angew. Chem. Int. Ed.*2016, 55, 5851-5855
Co-Pi-Fe_2O_3	~ 0.8	1.28	no	*J. Catal.*, 2017, 350, 48–55
IrO_2/RuO_2-Fe_2O_3	0.48	1.52	54 at at 1.25V (330 nm)	*Nano Energy* 2017, 38, 218–231
E−I−Sn−Fe_2O_3	~ 0.6	2.2	27 at 1.23V (330 nm)	*Nano Lett.*, 2017, 17, 2490–2495
Au-embedded α-Fe_2O_3	0.8	1.025	16 at 1.23V (410 nm)	*Chem.Commun.*, 2017,53, 4278-4281
Mg-Fe_2O_3/ Fe_2O_3 film	0.8	~ 0.5	19 at 1.0 V (300 nm)	*J. Am. Chem. Soc.* 2012, 134, 5508−5511

3 Reference

1. C. Li, A. Li, Z. Luo, J. Zhang, X. Chang, Z. Huang, T. Wang and J. Gong, *Angew. Chem. Internat. Edit.*, 2017, **129**, 4214-4219.
2. C. P. Wang Songcan, Yun Jung-Ho, Hu Yuxiang, Wang, Lianzhou, *Angew. Chem. Internat. Edit.*, 2017, **129**, 8620-8624.
3. M. D. Segall, J. D. L. Philip, M. J. Probert, C. J. Pickard, P. J. Hasnip, S. J. Clark and M. C. Payne, *J. Phys-Condens. Mat.*, 2002, **14**, 2717.
4. J. P. Perdew, K. Burke and M. Ernzerhof, *Phys. Rev. Lett.*, 1997, **78**, 3865.
5. D. R. Hamann, M. Schlüter and C. Chiang, *Phys. Rev. Lett.*, 1979, **43**, 1494-1497.
6. C. Li, J. S. Lian and Q. Jiang, *Phys. Rev. B*, 2011, **83**, 235125.
7. V. I. Anisimov, J. Zaanen and O. K. Andersen, *Phys. Rev. B*, 1991, **44**, 943.